Fast photolysis of carbonyl nitrates from isoprene

J.-F. Müller[1], J. Peeters[2], and T. Stavrakou[1]

[1]Belgian Institute for Space Aeronomy, Avenue Circulaire 3, 1180, Brussels, Belgium
[2]Department of Chemistry, University of Leuven, B-3001, Heverlee, Belgium

Abstract.

Photolysis is shown to be a major sink for isoprene-derived carbonyl nitrates, which constitute an important component of the total organic nitrate pool over vegetated areas. Empirical evidence from published laboratory studies on the absorption cross sections and photolysis rates of α-nitrooxy ketones suggests that the presence of the nitrate group (i) greatly enhances the absorption cross sections, and (ii) facilitates dissociation to a point that the photolysis quantum yield is close to unity, with O–NO$_2$ dissociation as a likely major channel. On this basis, we provide new recommendations for estimating the cross sections and photolysis rates of carbonyl nitrates. The newly estimated photorates are validated using a chemical box model against measured temporal profiles of carbonyl nitrates in an isoprene oxidation experiment by Paulot et al. (2009). The comparisons for ethanal nitrate and for the sum of methacrolein- and methylvinylketone nitrates strongly supports our assumptions of large cross section enhancements and a near-unit quantum yield for these compounds. These findings have significant atmospheric implications: the photorates of key carbonyl nitrates from isoprene are estimated to be typically between $\sim$3 and 20 times higher than their sink due to reaction with OH in relevant atmospheric conditions. Moreover, since the reaction is expected to release NO$_2$, photolysis is especially effective in depleting the total organic nitrate pool.

1 Introduction

Photolysis is recognized as a significant atmospheric sink for most oxygenated compounds generated in the oxidation of prominent non-methane volatile organic compounds such as isoprene. However, direct laboratory measurements of the photodissociation parameters are most often lacking, and

Correspondence to: J.-F. Müller (jfm@aeronomie.be)

model estimations must rely on analogies with structurally similar compounds for which those parameters are known from experiment. In the case of multifunctional organic compounds, it is common practice even in the most detailed chemical mechanisms (Saunders et al., 2003; Capouet et al., 2008) to treat each functionality independently of the other functional groups, i.e. the total photorate is calculated as a sum of independent contributions. Exceptions are provided by the cases of α-dicarbonyls, for which both cross section and quantum yield data is available (Atkinson et al., 2006; Sander et al., 2011), and α-nitrooxy ketones, for which cross sections were measured by Roberts and Fajer (1989) and Barnes et al. (1993). In both cases, interactions between the two neighbouring functional groups appear to strongly enhance the absorption cross sections. A similar effect is expected for α-nitrooxy aldehydes, but is not taken into account in models due to lack of data.

Regarding the photodissociation quantum yields of carbonyl nitrates, quite arbitrary assumptions are currently made in chemical mechanisms (Saunders et al., 2003; Xie et al., 2013) resulting in potentially large errors in the photolysis rates and product distributions. The difficulty resides in the large disparity between the quantum yield of monofunctional nitrates, usually assumed to be unity, independent of wavelength, and the quantum yield of carbonyls, which is very variable between different compounds, and frequently very low at atmospherically relevant wavelengths (i.e. above ca. 310 nm) (Atkinson et al., 2006). However, recent photorate measurements of several α-nitrooxy ketones in the laboratory (Suarez-Bertoa et al., 2012) appear to imply near-unit quantum yields for these compounds, and cast new light on the photodissociation process. Note that near-unit quantum yield in the photolysis of bifunctional carbonyls is not a novelty in itself: recent theoretical work (Peeters et al., 2009; Peeters and Müller, 2010) confirmed by laboratory experiments (Wolfe et al., 2012) has shown that isoprene-derived hydroperoxy enals (HPALDs) photodissociate with a quan-

tum yield of unity, i.e. more than two orders of magnitude higher than in the photolysis of monofunctional enones and enals such as methacrolein (MACR). Furthermore, photolysis was shown (theoretically and experimentally) to result in the breakup of the weakly bonded -OOH function and formation of OH radical. This example demonstrates that photon absorption by one chromophore in a multifunctional compound might cause rearrangement and dissociation in another part of the same molecule, that is in a sufficiently weakly bonded functional group. Examples of such groups are the hydroperoxide and peracid groups, but also – of relevance here – the nitro-oxy group, with its $RO–NO_2$ bond dissociation energy of only about 40 kcal mol^{-1}, similar to RO–OH.

Carbonyl nitrates constitute a sizeable fraction of the total pool of organic nitrates ($RONO_2$) over regions dominated by biogenic NMVOC emissions (Beaver et al., 2012). The role of organic nitrates as NOx reservoirs or sinks, and their importance to ozone production have been recognized (Perring et al., 2013). Differences in the model representation of their chemistry are estimated to cause substantial differences in model simulations of tropospheric ozone (Paulot et al., 2012) and other oxidants such as the hydroxyl radical OH. The photochemical lifetime and NOx recycling of these nitrates are therefore key parameters needed for an accurate description of tropospheric chemistry. Of particular relevance are several carbonyl nitrates known to be isoprene oxidation products identified in laboratory experiments (Paulot et al., 2009; Kwan et al., 2012) as well as in the field (Beaver et al., 2012; Perring et al., 2013). These compounds are listed in Table 1 along with their notation in the Master Chemical Mechanism (MCM) version 3.2 (Saunders et al., 2003). Note that the isomers MVKNO3, HMVKANO3 and MACRNO3 cannot be distinguished using current experimental techniques (Paulot et al., 2009; Beaver et al., 2012).

The α-nitrooxy carbonyls MVKNO3 and MACRNO3 are major second-generation nitrates formed in the oxidation of isoprene by OH, primarily through the OH- and O_3-oxidation of the β-hydroxy nitrates from isoprene (ISOPBO2 and ISOPDO2 in MCMv3.2). HMVKANO3 is a comparatively more minor nitrooxy ketone (Paulot et al., 2009). NC4CHO is a first-generation nitrate generated in the oxidation of isoprene by NO_3. α-Nitrooxy acetone (NOA) is likely the most abundant individual carbonyl nitrate (Beaver et al., 2012), due to its relatively long photochemical lifetime and because it is produced (as second or third generation product) in both the OH- and NO_3-initiated oxidation of isoprene (Xie et al., 2013).

In current mechanisms, low quantum yields are generally assumed for carbonyl nitrates (<0.3 above 310 nm for NOA in MCMv3.2), and NOA is often used as model compound for most α-nitrooxy carbonyls (including the aldehyde-nitrates), despite the much higher cross sections of (monofunctional) aldehydes compared to ketones in the atmospherically relevant wavelength range (Atkinson et al., 2006). As a result, the role of photolysis is very likely

strongly underestimated in models for those compounds. An improved assessment of this role is the main purpose of this study.

New recommendations for the estimation of the cross sections and photolysis quantum yields of carbonyl nitrates are presented in the next sections, based on the available evidence. A detailed isoprene oxidation mechanism largely based on MCMv3.2 is used in Sect. 4 to evaluate the impact of the new photorate estimation against the observed temporal evolution of products in the isoprene oxidation experiment at high NOx presented by Paulot et al. (2009). To that end, the rates of critical reactions of organic nitrates will be also reevaluated, given their importance in determining the temporal evolution of isoprene oxidation products. The atmospheric implications and conclusions of the new findings will be presented in Sect. 5 and Sect. 6.

2 Cross sections

We define the cross section enhancement r_{nk} of a carbonyl nitrate as the ratio of its absorption cross section (S_{nk}) to the sum of the cross sections of closely similar monofunctional compounds, namely a ketone k and a nitrate n (S_n and S_k):

$$r_{nk} = \frac{S_{nk}}{S_n + S_k} \tag{1}$$

Ideally, the monofunctional nitrate (n) should be the compound nk in which the ketone group is replaced by CH_2, and the ketone (k) should be the compound nk in which the nitrate group is replaced by a hydrogen. Note that as a general rule, $S_n \ll S_k$ at atmospherically relevant wavelengths (>310 nm).

The enhancement ratio r_{nk} is represented in Fig. 1 for three α-nitrooxy ketones, namely α-nitrooxy acetone, 3-nitrooxy-2-butanone and 1-nitrooxy-2-butanone, for which cross section measurements are available from Barnes et al. (1993). The cross sections of the following monofunctional compounds (obtained from Atkinson et al. (2006)) were used: acetone and n-propyl nitrate (for NOA), methylethylketone and i-propyl nitrate (for 3-nitrooxy-2-butanone), methylethylketone and n-propyl nitrate (for 1-nitrooxy-2-butanone). Note that i-propyl nitrate was used due to lack of data for $CH_3CH_2CH(ONO_2)CH_3$, which should not be of any consequence except at the shorter wavelengths, where S_n becomes dominant. Although it is difficult to assign error bars to the ratios shown on Fig. 1, the largest uncertainty likely concerns the cross sections (S_{nk}) of the nitrooxy-ketones. The uncertainty was estimated by Barnes et al. (1993) to be larger (80%) for NOA (due to its thermal instability) and for 1-nitrooxy-2-butanone (due to its relatively low vapor pressure) than for 3-nitrooxy-2-butanone (20%), but such a large difference between the two butanones does not appear justified by recent vapor pressure estimation methods (Compernolle et al., 2011). Note that

the cross sections of NOA measured in a previous laboratory study (Roberts and Fajer, 1989) were only slightly lower than those of Barnes et al. (1993), by about 12% on average between 310 and 330 nm.

Figure 1 clearly demonstrates a significant enhancement in the cross sections induced by the interaction between the two functional groups. The effect is especially pronounced in the cases of NOA and 3-nitrooxy-2-butanone, with $r_{nc} > 5$ for both compounds around 330 nm. Since the enhancement is largest at the higher wavelengths, where absorption by the nitrate chromophore is very small, it is clearly the absorption by the carbonyl chromophore which is enhanced due to the neighbouring nitrate group. This high sensitivity is expected: the forbidden nature of the (n,π^*) transition in carbonyls causes the transition probability (governed by the overlap of the ground state and excited state wave functions) to be very small but also very sensitive to even small changes in these wave functions, e.g. due to inductive or polarization effects by a neighbouring group such as ONO$_2$, due to its high electron affinity (E_a=3.94 eV). It follows that the enhancement seen for α-nitrooxy ketones is very likely a common feature for all α-nitrooxy carbonyls.

Given the absence of experimental data for α-nitrooxy aldehydes, we propose to calculate their absorption cross sections (S_{na}) following

$$S_{na} = (S_n + S_a) \cdot r_{nk} \qquad (2)$$

where S_n and S_a are measured cross sections of a monofunctional nitrate and a monofunctional carbonyl both structurally similar to the nitrooxy aldehyde under consideration, and r_{nk} is the enhancement ratio (Eq. 1) of a nitrooxy ketone (nk) most similar to na. This procedure is illustrated in Fig. 2 in the case of two isoprene-derived nitrooxy aldehydes, NO3CH2CHO and MACRNO3 (cf. Table 1). The monofunctional compounds used in this estimation are acetaldehyde and ethyl nitrate (for ethanal nitrate) and i-butyraldehyde and tert-butyl nitrate (for MACRNO3). The enhancement ratios of NOA and 3-nitrooxy-2-butanone (Fig. 1) were used for ethanal nitrate and MACRNO3, respectively. The impact of the cross section enhancement on the photolysis rates (J in s^{-1}) can be calculated with

$$J = \int \sigma(\lambda) \cdot q(\lambda) \cdot I(\lambda) \, d\lambda \qquad (3)$$

with λ the wavelength (nm), $\sigma(\lambda)$ (cm^2 molec^{-1}) and $q(\lambda)$ the cross section and quantum yield, and $I(\lambda)$ the actinic flux (quanta cm^{-2}s^{-1} nm^{-1}). Assuming wavelength-independent quantum yields, and using the Tropospheric Ultraviolet and Visible (TUV) model from NCAR (Madronich, 1993) (for overhead sun, 348 DU ozone), the J-values of NO3CH2CHO and MACRNO3 are increased by factors of about 3 and 4, respectively, compared to a calculation using $S_{na} = (S_n + S_a)$.

The inductive effects of a nitrate group are expected to decrease when the distance between the functional groups increases, as observed e.g. in the well-documented effect of ONO$_2$ on neighbouring C-H bonds (Neeb, 2000). In absence of experimental data for β-nitrooxy carbonyls, we'll assume that their cross sections are also significantly affected by the presence of the nitrate group, if only more moderately (assumed factor of 2 increase).

Note that the presence of a hydroxy group (as often found in isoprene-derived nitrates) is known to have also a significant, although variable effect on the cross sections of both carbonyls (Messaadia et al., 2012) and nitrates (Roberts and Fajer, 1989). This effect will be generally neglected here for the sake of simplicity, although its possible significance will be briefly discussed in Sect. 4.4.

Although very uncertain, considering the wide range of enhancement ratios observed for different nitrooxy-ketones (Fig. 1), the high photorates implied by the procedure above in combination with the quantum yield estimates discussed in the next Section appear consistent with the nitrooxy carbonyl measurements in the isoprene oxidation experiment of Paulot et al. (2009), as shown in Sect. 4.

3 Quantum yields

Using high pressure Xenon arc lamps as irradiation source in the indoor simulation chamber CESAM, Suarez-Bertoa et al. (2012) determined the photolysis rates of three α-nitrooxy ketones, including two compounds (α-nitrooxyacetone and 3-nitrooxy-2-butanone) for which the absorption cross sections are known (Barnes et al., 1993). On this basis, near-unit quantum yields were inferred for these compounds (Suarez-Bertoa et al., 2012). Using Eq. 3 with the lamp spectrum and NO$_2$ photolysis rate given in Suarez-Bertoa et al. (2012), we estimate the average quantum yield to be 0.9 for NOA and 0.75 for 3-nitrooxy-2-butanone, with an estimated error of ca. 0.2. The value of 0.9 is a factor of 4 higher than the MCMv3.2 averaged quantum yield for NOA, weighted by the cross section and actinic flux for overhead sun, surface conditions. Also for comparison, the (weighted) average quantum yield of the simple ketones acetone (Blitz et al., 2004) and methylethylketone (Baeza-Romero et al., 2005) are 0.06 and 0.25, respectively. Even much lower values (<0.01) were determined for enones and enals, such as methylvinylketone (MVK) and methacrolein (MACR) (Sander et al., 2011; Pinho et al., 2005).

The near-unity quantum yield of nitrooxy-ketones can be rationalized by mechanisms similar to that proposed for the hydroperoxy enals HPALDs (Peeters and Müller, 2010). Photon absorption by the carbonyl chromophore yielding the excited S1 state and fast intersystem crossing (ISC) to the triplet T1 state may be followed, via spin exchange, by avoided crossing of the T1 surface with the repulsive T2 surface of the O-NO$_2$ chromophore, resulting in fast dissociation of the weak (ca. 40 kcal/mol) O-NO$_2$ bond. Alternatively, a chemical rearrangement of the excited T1 state may

lead to either indirect dissociation to the same final products, or to multistep decomposition yielding NO, a carbonyl and an acyloxy radical. Another possible mechanism is internal conversion (IC) of the initially excited singlet state S1 to the ground state S0, followed by prompt dissociation of the weakest bond, i.e. O-NO$_2$, due to the high vibrational energy. Indeed, in the photodissociation dynamics of ketones, IC of S1 to S0 is expected to compete effectively with ISC of S1 to the triplet T1 state (Favero et al., 2013). Due to the competition with collisional stabilisation, this latter mechanism can only be effective for molecules that are not too large, allowing dissociation on the S0 surface still faster than $10^9 s^{-1}$.

In any case, a quantum yield not much below unity is likely also for other carbonyl nitrates, including the β-nitrooxy ketone and nitrooxy aldehydes of Table 1, in particular the enal NC4CHO structurally very similar to HPALDs (replacing ONO$_2$ by a hydroperoxy group). For simplicity, we'll assume a value of unity in the calculations presented in the next section, and O–NO$_2$ breakup will be assumed to be the only photolysis channel considered. Typical photolysis rates of key carbonyl nitrates from isoprene implied by the above recmmendations for cross sections and quantum yields are given in Table 3.

4 Evaluation against isoprene oxidation experiment of Paulot et al. (2009)

Thanks to the Chemical Ionisation Mass Spectrometry (CIMS) technique, a wide range of products could be monitored in the isoprene oxidation experiment of Paulot et al. (2009), although interpretation is made difficult by the possible confusion between different isobaric compounds contributing to the same signal. With that limitation in mind, Paulot et al. (2009) analyzed the different signals to constrain a large number of mechanistic parameters (branching ratios and kinetic rates) in a detailed, quasi-explicit chemical mechanism. To a large extent, those new constraints are adopted in the mechanism described in the next subsection. The photolysis of organic nitrates was however essentially neglected by Paulot et al. (2009), since the very low photorates of simple alkyl nitrates ($<10^{-6}$ s^{-1} in the Caltech chamber) were adopted for carbonyl nitrates. Reaction with OH being the only other sink for those compounds, their rates adjusted by Paulot et al. (2009) on the basis of the CIMS signals were found to be substantially overestimated compared to both Structure-Activity-Relationships (SARs) (e.g., Neeb (2000)) and, in the case of the nitrooxy-ketones, recent laboratory measurements for very similar compounds (Suarez-Bertoa et al., 2012). A reevaluation of the respective roles of photolysis and OH-oxidation of carbonyl nitrates is therefore clearly needed.

The experiment was conducted at high NOx using H$_2$O$_2$ photolysis as OH source, with J(H$_2$O$_2$)=3.1·10^{-6} s^{-1}. The lamps are blacklights (GE350BL) irradiating above 300 nm,

with a maximum at 354 nm (Kroll et al., 2006; Cocker et al., 2001). Initial conditions are 500 ppbv NO, 94 ppbv isoprene and 2.1 ppmv H$_2$O$_2$. Our chemical box model uses the Kinetic Pre-Processor (KPP) package (Sandu et al., 2006) with its embedded Rosenbrock solver of order 4.

4.1 General lines of isoprene mechanism

The chemical degradation mechanism of isoprene at high NO is largely based on the MCMv3.2 (http://mcm.leeds.ac.uk/MCM/), with a number of updates. Inorganic reaction rates were revised based on the JPL recommendation (Sander et al., 2011).

Due to the high initial NO level and moderate temperatures (291.5–296.5 K) in the experiment of Paulot et al. (2009), the isomerisation reactions proposed by Peeters et al. (2009) for Z-δ-hydroxyperoxy radicals from isoprene + OH and by Crounse et al. (2012) for β-hydroxyperoxy radicals from MACR + OH were both too slow (of the order of 1 s^{-1} or less) to compete with their reaction with NO, and are therefore neglected here. The only non-negligible unimolecular reactions of the isoprenyl peroxy radicals are their O$_2$ loss reactions, with rates of the order of 10 s^{-1} for the least stable radical (at 292 K, the temperature prevailing in the isoprene consumption stage which lasted 20 minutes) (Peeters and Müller, 2010). Because the Z-δ-hydroxy peroxys from isoprene decompose faster than their β-hydroxy counterparts, the net effect of the O$_2$-elimination and re-addition reactions is to increase the yield of β-hydroxy peroxy products such as MVK, MACR and the β-hydroxynitrates, at the expense of the δ-hydroxyperoxy products, including the δ-hydroxynitrates. Although this effect is estimated to be substantial in atmospheric conditions, as it reduces the δ-hydroxyperoxy product yield by an order of magnitude (Peeters and Müller, 2010), it is very small at the high NO levels of Paulot et al. (2009) and is therefore not considered here.

We adopt the MCMv3.2 branching ratios for the formation of the different hydroxyperoxy radicals from isoprene+OH, which include the β-hydroxyperoxys ISOPBO2 and ISOPDO2 and the δ-hydroxyperoxys ISOPAO2 and ISOPCO2 (Table 2). Note that OH-addition to the central carbons of isoprene is ignored, as it represents only about 7% of the total (Park et al., 2004). Whereas the overall nitrate yield in the reaction of first-generation isoprene peroxys with NO is relatively well constrained (8±3%) by experimental data (Atkinson et al., 2006), the yields of individual nitrates are much more uncertain (Orlando and Tyndall, 2012). We adopt here the yields derived by Paulot et al. (2009): 6.7% for the β-hydroxyperoxys and 24% for the δ-hydroxyperoxys, slightly higher than in a previous experimental study (Giacopelli et al., 2005). Note that those much higher yields for δ- compared to β-hydroxyperoxys appear to be at odds with previous findings showing that 1,4-substitutions tend to reduce the nitrate yield, as discussed by Orlando and Tyn-
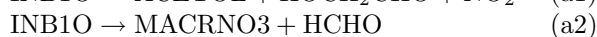
dall (2012). An alternative choice (8%) for the yield of δ-hydroxynitrates will be therefore also tested with the model.

4.2 Pathways to carbonyl nitrates

Carbonyl nitrates are formed from both the further degradation of the first-generation hydroxynitrates (see below) and the oxidation of the major products MVK and MACR by OH and O_3. MACRNO3 is e.g. formed from OH addition to the external carbon of the double bond in MACR, followed by O_2 addition and reaction with NO. MVKNO3 (HMVKANO3) is formed from the major (minor) OH addition to MVK, namely to the external (internal) carbon of the double bond, followed by O_2 addition and NO-reaction. We adopt here the nitrate yields in those NO-reactions estimated by Paulot et al. (2009) : 15% for MACRNO3 and 11% for MVKNO3+HMVKANO3, consistent with a previous laboratory study (Chuong and Stevens, 2004). The branching ratio for addition to the terminal carbon of MVK is 85%, based on the SAR of Peeters et al. (2007), as validated for similar enone compounds by Orlando et al. (1999) and Orlando and Tyndall (2002).

The first-generation hydroxynitrates from isoprene can undergo reaction with OH and O_3, whereas photolysis is very slow (ca. 10^{-6} s^{-1} or less). According to MCMv3.2, the ozonolysis of each major hydroxynitrate (ISOPANO3, ISOPBNO3, ISOPCNO3 and ISOPDNO3) generates a different carbonyl nitrate (NO3CH2CHO, MACRNO3, NOA and MVKNO3, respectively) at overall yields of 0.55–0.6. Since, as will be shown in Sect. 4.3, the reaction with ozone plays only a minor role in the experimental conditions of Paulot et al. (2009), the following discussion focuses on the OH-degradation mechanism.

OH addition to ISOPBNO3 and ISOPDNO3 proceeds primarily by terminal addition (85%) (Peeters et al., 2007), followed by O_2 addition to the internal C. The NO-reaction of the resulting peroxy radicals (INB1O2 from ISOPBNO3 and INDO2 from ISOPDNO3, see Table 2) generates oxy radicals (INB1O and INDO), each decomposing following two possible pathways:

$$INB1O \rightarrow ACETOL + HOCH_2CHO + NO_2 \quad (a1)$$
$$INB1O \rightarrow MACRNO3 + HCHO \quad (a2)$$
and
$$INDO \rightarrow ACETOL + HOCH_2CHO + NO_2 \quad (b1)$$
$$INDO \rightarrow MVKNO3 + HCHO \quad (b2)$$

We adopt the branching ratios proposed by Paulot et al. (2009) consistent with their experimental results: 60% for both (a1) and (b1). Note that in MCMv3.2, path (a2) is ignored, and (b2) is largely dominant ($\sim$90%). For both oxy radicals, the difference between the SAR-predicted barrier heights (Vereecken and Peeters, 2009) for the two possible channels is small (1–2 kcal mol^{-1}) implying that H-bonding effects – not accounted for in the SAR but possibly exceeding 2 kcal mol^{-1} – could decide the real branching fractions.

Upon OH/O_2 addition to ISOPANO3, reaction with NO of the resulting peroxy radical INAO2 (Table 2) forms an oxy radical decomposing to hydroxyacetone and (upon O_2 addition) an α-hydroxyperoxy radical HOCH(O_2)CH2(ONO2) expected to readily eliminate HO2 and thus form ethanal nitrate. An additional decomposition pathway (to HCHO+HCOOH+NO3), representing 70% of the total, was invoked by Paulot et al. (2009) in order to reduce the yield of ethanal nitrate and match its measured concentrations in their experiment. This unusually involved pathway must be invoked only under the assumption of a high nitrate yield (0.24) in the reaction of δ-peroxynitrates with NO. It is therefore not considered in model runs assuming a low nitrate yield (8%).

Finally, the reaction with NO of the peroxy radical (INCO2) formed upon OH/O_2 addition to ISOPCNO3 produces an oxy radical decomposing to NOA and glycolaldehyde. The alternative pathway proposed by Paulot et al. (2009), i.e. decomposition to dihydroxybutanone+HCHO+NO2 is predicted to face a ca. 8 kcal mol^{-1} higher barrier (Vereecken and Peeters, 2009) and is therefore neglected.

4.3 Constraining the OH- and O_3 reaction rates of the β-hydroxynitrates from isoprene

Paulot et al. (2009) inferred a low OH-addition rate constant for the β-hydroxynitrates, $1.3 \cdot 10^{-11}$ cm^3 molec.$^{-1}$ s^{-1}, found necessary to match the evolution of the CIMS signal of the isoprene hydroxynitrates. It is unclear why this rate is so different from the OH-addition rate to the δ-hydroxy nitrates, $9.5 \cdot 10^{-11}$ in Paulot et al. (2009) and $6.9 \cdot 10^{-11}$ cm^3 molec.$^{-1}$ s^{-1} in MCMv3.2. We adopt the MCMv3.2 value for the δ-hydroxynitrates; the precise value was found to have little influence on the modeling results.

Although ozonolysis is relatively unimportant for the δ-hydroxynitrates due to their high reactivity towards OH (Paulot et al., 2009), it might play a significant, yet uncertain role for the β-hydroxynitrates. Rates of the order of 10^{-17} cm^3 molec.$^{-1}$ s^{-1} were assumed by Giacopelli et al. (2005) and Paulot et al. (2009) based on previous measurements for terminal alkenes. However, a much higher ozonolysis rate was recently determined in the laboratory by Lockwood et al. (2010) for the 1,2-hydroxynitrate ISOPBNO3 ($10.6 \cdot 10^{-17}$ cm^3 molec.$^{-1}$ s^{-1}), about twice higher than the measured rate for the 1,4-hydroxynitrate ISOPCNO3 ($5.3 \cdot 10^{-17}$ cm^3 molec.$^{-1}$ s^{-1}). Those values were adopted in MCMv3.2 and in recent global model studies (Xie et al., 2013; Mao et al., 2013) for all isoprene β- and δ-hydroxynitrates, respectively.

Fig. 3 shows the calculated time profiles of isoprene, OH radical and ozone in the isoprene oxidation experiment. Those results are very similar to the modeling results of Paulot et al. (2009). Isoprene is entirely consumed within the first two hours. Whereas OH concentrations show only moderate variations, ranging between 0.2 and 0.3 pptv (or
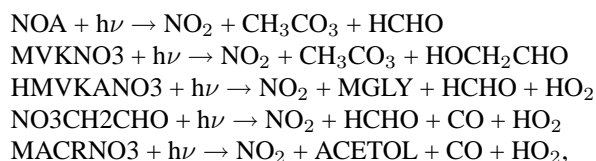
about 5 and $7 \cdot 10^6$ molec. cm^{-3}), ozone is predicted to increase continuously from near-zero to about 500 ppbv after 10 hours. Owing to their short chemical lifetime (<1 hour), the δ-hydroxynitrates are expected to be consumed within the first four hours. At later times, the temporal profile of the isoprene hydroxynitrates (Fig. 4) is controlled solely by the reactions of the β-hydroxynitrates with OH and O$_3$. In the first hours, however, the profile is also dependent on the respective yields of β- versus δ-hydroxynitrates. For this reason, we show model results obtained using either a high (Y_δ=0.24) or low (Y_δ=0.08) value for the nitrate yield in the reaction of δ-hydroxyperoxys with NO.

In the first case (left panel of Fig. 4), the sensitivity calculations are fully consistent with the conclusions of Paulot et al. (2009): the best results are obtained when using low values for both rate coefficients of the β-hydroxynitrates: $k_{OH} = 1.3 \cdot 10^{-11}$ and $k_{O3} = 1 \cdot 10^{-17}$ cm^3 molec.$^{-1}$ s^{-1}. Adopting the very high ozonolysis rate by Lockwood et al. (2010) (VH run) leads to an almost complete disappearance of the hydroxynitrates after only 4 hours due to the short chemical lifetime (<30 minutes after 4 hours of experiment) implied by the high reaction rate. The chemical sink after 6 hours is overestimated by more than a factor 5 in this simulation. Even a moderately high ozonolysis rate of $3 \cdot 10^{-17}$ cm^3 molec.$^{-1}$ s^{-1} is clearly incompatible with the data. As seen in Fig. 4, these conclusions are independent on the choice of Y_δ and should therefore be considered as robust.

When a low yield of δ-hydroxynitrates is adopted, the best results are obtained when using a higher OH-reaction rate for the β-hydroxynitrates ($2.2 \cdot 10^{-11}$ cm^3 molec.$^{-1}$ s^{-1}), which compensates for the lower share of the short-lived δ-hydroxynitrates to the CIMS signal in the first hours of the experiment. As a result of the higher k_{OH}, the profile shape at later times requires a further lowering of the ozonolysis rate, explaining the better agreement obtained in the simulation using the lowest value for k_{O3} ($0.5 \cdot 10^{-17}$ cm^3 molec.$^{-1}$ s^{-1}).

4.4 Sinks of carbonyl nitrates: photolysis vs. OH-reaction

The (saturated) carbonyl nitrates from isoprene can undergo photolysis and H-abstraction by OH radicals. Photolysis is assumed to eliminate NO$_2$. Merging the initial photolysis reaction with the fast subsequent unimolecular reaction of the oxy co-product (and possibly reaction with O$_2$) yields

NOA + hν → NO$_2$ + CH$_3$CO$_3$ + HCHO
MVKNO3 + hν → NO$_2$ + CH$_3$CO$_3$ + HOCH$_2$CHO
HMVKANO3 + hν → NO$_2$ + MGLY + HCHO + HO$_2$
NO3CH2CHO + hν → NO$_2$ + HCHO + CO + HO$_2$
MACRNO3 + hν → NO$_2$ + ACETOL + CO + HO$_2$,

where MGLY denotes methylglyoxal. The photolysis reactions of the other carbonyl nitrates generated in the oxidation of isoprene are given in the Supplement to this article. The

OH-oxidation mechanism is obtained from MCMv3.2. The OH-reaction rates are taken either from the SAR of Neeb (2000) or from the MCMv3.2, itself based on previous SARs. In both cases, the rates are substantially lower than the values determined by Paulot et al. (2009) for NO3CH2CHO, MACRNO3 and MVKNO3 based on the CIMS profiles, very likely due the underestimation of photolysis in their analysis. The analysis by Neeb (2000) of kinetic measurements for a large number of alkyl nitrates indicates that the presence of the ONO$_2$ group reduces drastically the H-abstraction rate on both α- and β-carbons. The OH-reaction rates of three nitrooxy-ketones, namely α-nitrooxyacetone, 3-nitrooxy-2-butanone and 3-methyl-3-nitrooxy-2-butanone, were measured recently by Suarez-Bertoa et al. (2012), with values, in units of 10^{-12} cm^3 molecule^{-1} s^{-1}, of 0.67±0.25, 1.06±0.41 and 0.26±0.09, respectively. These values fall between the estimates by Neeb (2000) (0.58, 0.68 and 0.24, respectively) and the MCMv3.2 (1.0, 1.2 and 0.34). These SAR estimates always lie within the experimental error bars, except in the case of MCMv3.2 for NOA.

The difference between MCMv3.2 and Neeb (2000) is large in the case of nitrooxy-aldehydes, e.g. for ethanal nitrate NO3CH2CHO: $k_{OH} = 1.2 \cdot 10^{-12}$ (Neeb) vs. $3.4 \cdot 10^{-12}$ cm^3 molecule^{-1} s^{-1} (MCM). Nevertheless, the impact of this difference is relatively small on the modeled temporal profile of NO3CH2CHO, as seen on Fig.5. Whichever SAR estimate is used for the OH-reaction rate, the low photorate estimated by MCM ($J_{MCM} = 1.7 \cdot 10^{-6}$ s^{-1}) leads to a strong underestimation of the decay of NO3CH2CHO after the concentration peak, i.e. at times $t > 2$–3 hours. In contrast, the high photolysis rate ($J_{fast} = 4.4 \cdot 10^{-5}$ s^{-1}) calculated using enhanced absorption cross sections (Sect. 2) and a unit quantum yield leads to a far better agreement with the observed temporal profile. More precisely, a near-perfect fit at $t > 5$ hours is obtained when adopting either k_{OH} from Neeb (2000) and $J = J_{fast}$, or k_{OH} from MCMv3.2 and $J = 0.75 \cdot J_{fast}$ (not shown on the figure). The measurements therefore validate both the strongly enhanced cross sections (Sect. 2) and the assumption of a near-unit quantum yield (Sect. 3) for ethanal nitrate.

The choice of the OH-reaction SAR (Neeb or MCM) has very little influence on the temporal profile shape of the methylvinylketone- and methacrolein nitrates (MVKNO3+HMVKANO3+MACRNO3), as seen on Fig. 6. As for ethanal nitrate, the simulations assuming a fast photolysis of carbonyl nitrates provide a better match with the observed temporal profile. The model results appear to be further improved by the use of a higher OH-reaction rate of β-hydroxynitrates (Fig. 6(b)) which was found consistent with the hypothesis of a low yield of δ-hydroxynitrates (see Fig. 4). Reasons for the remaining discrepancy between the model and the CIMS measurements might be multiple, including e.g. still underestimated photolysis rates, or an underestimated production rate of the short-lived MACRNO3 compared to the comparatively longer-lived MVKNO3 and

HMVKANO3. For example, an excellent agreement with the data (r^2=0.99) can be achieved by doubling the photolysis rates of all three compounds.

Higher photorates for MVKNO3 and MACRNO3 might be explained by the effect of their hydroxy group in beta position, as shown by the higher cross sections of the β-hydroxy ketone $CH_3C(O)CH_2CH_2OH$ (Messaadia et al., 2012) compared to methylethyl-ketone MEK (Atkinson et al., 2006) above 320 nm. Although measurement uncertainties might be significant at those wavelenghts, the observed strong enhancement (exceeding a factor of 5 above 330 nm) might be explained by (i) a red-shift in the cross sections due to a lowering of the energy difference between the ground state S0 and the excited state S1, resulting from a stronger H-bond in S1 compared to S0 between the carbonyl-O and the hydroxy-H, and (ii) the so-called hot bands, i.e. excitations of vibrationally excited levels of S0, expected near the 0 K band-limit (ca. 335 nm). The significance of the latter effect is made clear by the case of 3-hydroxy 3-methyl 2-butanone: its cross sections were found by Messaadia et al. (2012) to be almost an order of magnitude higher than those of 3-hydroxy 2-butanone around 335 nm, indicating that the increased number of low-frequency vibration modes due to the additional CH_3 group causes a substantially increased absorption near the 0 K band-limit.

In contrast, the presence of a hydroxy group in alpha position in HMVKANO3 is expected to decrease its cross sections, based on the measured cross sections of hydroxyacetone (Atkinson et al., 2006) and 3-hydroxy 2-butanone (Messaadia et al., 2012). Nonetheless, since this compound represents only a minor (<10%) fraction of the sum MVKNO3+HMVKANO3+MACRNO3, the overall impact of the hydroxy group on the photolysis rates is very likely a significant enhancement, consistent with the above model results.

5 Atmospheric implications

Photolysis is found to be, by far, the dominant sink of isoprene-derived carbonyl nitrates in relevant atmospheric conditions, as seen in Table 3. Adopting a concentration of OH ($5 \cdot 10^6$ molec. cm^{-3}) typically measured during daytime over Amazonia (Lelieveld et al., 2008) and the Eastern United States in summer (Ren et al., 2008), the clear-sky photorates are estimated to be between $\sim$3 and 20 times higher than the sink due to reaction with OH, even when neglecting hydroxy group effects. This has important consequences regarding the role of isoprene nitrate formation on the budget of NOx because, whereas photolysis is expected to release NO_2, the nitrate group is very often retained in the reaction of carbonyl nitrates with OH, leading to a variety of compounds including aldehydes, peroxyacyl nitrates and hydroperoxides, all bearing the nitrate group. Needless to say, the subsequent degradation of those compounds is complex

and uncertain, and therefore difficult to represent in large-scale models. Photolysis, on the other hand, is more effective in depleting the total organic nitrate pool, and it leads to a generally much simpler chemistry, as seen in the cases of the isoprene nitrates considered in Sect. 4.4. The dominance of photolysis as a sink for carbonyl nitrates, and particularly for the α-nitrooxy aldehydes (Table 3) should therefore facilitate the elaboration of reduced chemical mechanisms for use in large-scale models.

The estimated lifetimes of the key secondary isoprene nitrates (Table 3) can be compared to the lifetime of the first-generation β-hydroxynitrates from isoprene, between 2.4 and 3.8 hours (assuming 35 ppbv O_3 and $5 \cdot 10^6$ molec. cm^{-3} OH, and using k_{OH} and k_{O3} determined in Sect. 4.3). The δ-hydroxynitrates are comparatively much shorter-lived (0.5 hour) but are expected to be unimportant in atmospheric conditions, because their yields are predicted to be reduced by about one order of magnitude due to the fast interconversion of isoprene hydroxyperoxys (Peeters and Müller, 2010). Note that this yield reduction is consistent with the absence of atmospheric measurements for the C_5-hydroxyaldehydes (produced alongside the δ-hydroxynitrates) known to be formed in high yields in the oxidation of isoprene by OH at very high NO (Atkinson et al., 2006). From these considerations, and since nitrooxy acetone is essentially not formed from the β-hydroxy pathways, the photochemical lifetime of the major secondary nitrates from isoprene+OH in atmospheric conditions (i.e. mostly MVKNO3 and MACRNO3) is estimated to be relatively similar, or even possibly lower, than the lifetime of the first-generation (β-)hydroxynitrates. This is broadly consistent with the CIMS measurements of primary and secondary isoprene nitrates during the BEARPEX 2009 campaign in California, which indicate about twice higher concentrations of first-generation hydroxynitrates compared to second-generation nitrates (Beaver et al., 2012). In contrast, a Lagrangian model study (Perez et al., 2009) using an updated version of MCMv3.1 predicted that second-generation nitrates should be about 6 times more abundant than the first-generation hydroxynitrates, due to the assumed high reactivity of the latter and neglected photolysis of the former.

6 Conclusions

Interactions between functional groups were shown to play a crucial role in the photolysis of carbonyl nitrates. The nitrate group appears to (1) enhance photon absorption by the carbonyl chromophore, and (2) facilitate dissociation upon photon absorption, to a point that the quantum yield is close to unity, with O–NO_2 dissociation as the likely major (or only) photolysis channel. We tentatively quantified these effects using existing laboratory data for the cross sections (Barnes et al., 1993) and photolysis rates (Suarez-Bertoa et al., 2012) of specific α-nitrooxy ketones. In absence of direct measure-

ments of photolysis parameters for nitrooxy aldehydes, our recommended photorate estimation has a potentially large uncertainty for those compounds. Fortunately, an unexpected validation is provided in the case of ethanal nitrate, the simplest nitrooxy aldehyde, by its CIMS temporal profile in the isoprene oxidation experiment of Paulot et al. (2009), as it implies a strong sink besides OH-reaction, consistent with our assumptions regarding the photolysis parameters. Photolysis is also shown to be a major sink for the key secondary nitrates MVKNO3 and isomers. A further enhancement of their cross sections due to their hydroxy group (in beta position in MVKNO3 and MACRNO3) is also supported by the model comparisons.

Given the noted importance of carbonyl nitrate photolysis for the budget of NOx and therefore ozone in the troposphere, the need for additional laboratory data should be acknowledged. For example, absorption cross section measurements for (1) α-nitrooxy aldehydes and (2) β-nitrooxy carbonyls would be especially helpful in order to validate and refine the above conclusions. Also, cross section enhancement effects might exist for other bifunctional carbonyls, including hydroperoxides and peracids, and should be explored. A reduced chemical mechanism incorporating those effects should be elaborated and implemented in atmospheric chemistry models, in order to evaluate the impact of mechanistic assumptions and rate estimations against field campaigns.

References

Atkinson, R., D. L. Baulch, R. A. Cox, J. L. Crowley, R. F. Hampson, R. G. Hynes, M. E. Jenkin, M. J. Rossi, and J. Troe: Evaluated kinetic and photochemical data for atmospheric chemistry: Volume II – gas phase reactions of organic species, Atmos. Chem. Phys., 6, 3625–4055, 2006.

Baeza-Romero, M. T., M. A. Blitz, D. E. Heard, M. J. Pilling, B. Price, P. W. Seakins, and L. Wang: Photolysis of methylethyl, diethyl and methylvinyl ketones and their role in the atmospheric HOx budget, Faraday Discuss., 130, 73–88, 2005.

Barnes, I., K. H. Becker, and T. Zhu: Near UV absorption spectra and photolysis products of difunctional organic nitrates: Possible importance as NOx reservoirs, J. Atmos. Chem. 17, 353–373, 1993.

Beaver, M. R., J. M. St. Clair, F. Paulot, K. M. Spencer, J. D. Crounse, B. W. LaFranchi, K. E. Min, S. E. Pusede, P. J. Wooldridge, G. W. Schade, C. Park, R. C. Cohen, and P. O. Wennberg: Importance of biogenic precursors to the budget of organic nitrates: observations of multifunctional organic nitrates by CIMS and TD-LIF during BEARPEX 2009, Atmos. Chem. Phys., 12, 5773–5785, 2012.

Blitz, M. A., D. E. Heard, and M. J. Pilling: Pressure and temperature-dependent quantum yields for the photodissociation of acetone between 279 and 327.5 nm, Geophys. Res. Lett., 31, L06111, doi:10.129/2003GL018793, 2004.

Capouet, M., J.-F. Müller, K. Ceulemans, S. Compernolle, L. Vereecken, and J. Peeters: Modeling aerosol formation in alpha-pinene oxidation experiments, J. Geophys. Res., 113, D02308, doi:10.1029/2007JD008995, 2008.

Chuong, B., and P. S. Stevens: Measurements of the kinetics of the OH-initiated oxidation of methyl vinyl ketone and methacrolein, Int. J. Chem. Kin., 36, 12—25, 2004.

Cocker, D. R., R. C. Flagan, and J. H. Seinfeld: State-of-the-art chamber facility for studying atmospheric aerosol chemistry, Environ. Sci. Technol., 35, 2594–2601, 2001.

Compernolle, S., K. Ceulemans, and J.-F. Müller: EVAPORATION: a new vapor pressure estimation method for organic molecules including non-additivity and intramolecular interactions, Atmos. Chem. Phys., 19431–9450, 2011.

Crounse, J. D., F. Paulot, H. G. Kjaergaard, and P. O. Wennberg: Peroxy radical isomerisation in the oxidation of isoprene, Phys. Chem. Chem. Phys., 13, 13607–13613, 2011.

Crounse, J. D., H. C. Knap, K. B. Ørnsø, S. Jørgensen, F. Paulot, H. G. Kjaergaard, and P. O. Wennberg: Atmospheric fate of methacrolein. 1. Peroxy radical isomerization following addition of OH and O2, J. Phys. Chem., 116, 5756–5762, 2012.

Favero, L., G. Granucci, and M. Persico: Dynamics of acetone photodissociation: a surface hopping study, Phys. Chem. Chem. Phys., 15, 20651–20661, 2013.

Giacopelli, P., K. Ford, C. Espada, and P. B. Shepson: Comparison of the measured and simulated isoprene nitrate distributions above a forest canopy, J. Geophys. Res., 110, D01304, doi:10.1029/2004JD005123, 2005.

Kroll, J. H., N. L. Ng, S. M. Murphy, R. C. Flagan, and J. H. Seinfeld: Secondary organic aerosol formation from isoprene photooxidation, Environ. Sci. Technol., 40, 1869–1877, 2006.

Kwan, A. J., A. W. H. Chan, N. L. Ng, H. G. Kjaergaard, J. H. Seinfeld, and P. O. Wennberg: Peroxy radical chemistry and OH radical production during the NO3-initiated oxidation of isoprene, Atmos. Chem. Phys., 12, 7499–7515, 2012.

Lelieveld, J., T. M. Butler, J. N. Crowley, T. J. Dillon, H. Fischer, L. Ganzeveld, H. Harder, M. G. Lawrence, M. Martinez, D. Taraborrelli, and J. Williams : Atmospheric oxidation capacity sustained by a tropical forest, Nature, 452, 737–740, 2008.

Lockwood, A., P. B. Shepson, M. N. Fiddler, and M. Alaghmand: Isoprene nitrates: preparation, separation, identification, yields, and atmospheric chemistry, Atmos. Chem. Phys., 10, 6169–6178, 2010.

Madronich, S.: UV radiation in the natural and perturbed atmosphere, in Environmental Effects of Ultraviolet Radiation, edited by M. Tevini, pp. 17–69, Lewis, Boca Raton, Florida, 1993.

Mao, J., F. Paulot, D. J. Jacob, R. C. Cohen, J. D. Crounse, P. O. Wennberg, C. A. Keller, R. C. Hudman, M. P. Barkley, and L. W. Horowitz: Ozone and organic nitrates over the eastern United States: Sensitivity to isoprene chemistry, J. Geophys. Res., 118, doi:10.1002/jgrd.50817, 2013.

Messaadia, L., G. El Dib, A. Ferhati, E. Roth and A. Chakir: Gas phase UV absorption cross-sections for a series of hydroxycarbonyls, Chem. Phys. Lett., 529, 16-22, 2012.

Neeb, P.: Structure-Reactivity based estimation of the rate constants for hydroxyl radical reactions with hydrocarbons, J. Atmos. Chem., 35, 295–315, 2000.

Orlando, J. J., G. S. Tyndall, and S. E. Paulson: Mechanism of the OH-initiated oxidation of methacrolein, Geophys. Res. Lett., 26,

2191–2194, 1999.

Orlando, J. J., and G. S. Tyndall: Mechanism for the reaction of OH with two unsaturated aldehydes: Crotonaldehyde and acrolein, J. Phys. Chem., 106, 12252–12259, 2002.

Orlando, J. J., and G. S. Tyndall: Laboratory studies of organic peroxy radical chemistry: an overview with emphasis on recent issues of atmospheric significance, Chem. Soc. Rev., 41, 6294–6317, 2012.

Park, J., C. G. Jongsma, R. Zhang, and S. W. North: OH/OD initiated oxidation of isoprene in the presence of O_2 and NO, J. Phys. Chem., 108, 10688–10697, 2004.

Paulot, F., J. D. Crounse, H. G. Kjaergaard, J. H. Kroll, J. H. Seinfeld, and P. O. Wennberg: Isoprene photooxidation: new insights into the production of acids and organic nitrates, Atmos. Chem. Phys., 9, 1479–1501, 2009.

Paulot, F., D. K. Henze, and P. O. Wennberg: Impact of the isoprene photochemical cascade on tropical ozone, Atmos. Chem. Phys., 12, 1307–1325, 2012.

Peeters, J., W. Boullart, V. Pultau, S. Vandenberk, and L. Vereecken: Structure-Activity Relationship for the addition of OH to (poly)alkenes: Site-specific and total rate constants, J. Phys. Chem., 111, 1618–1631, 2007.

Peeters, J., T. L. Nguyen, and L. Vereecken: HOx radical regeneration in the oxidation of isoprene, Phys. Chem. Chem. Phys., 11, 5935–5939, doi:10.1039/b908511d, 2009.

Peeters, J., and J.-F. Müller: HOx radical regeneration in isoprene oxidation via peroxy radical isomerisations. II: Experimental evidence and global impact, Phys. Chem. Chem. Phys., 12(42), 14227–14235, doi:10.1039/C0CP00811G, 2010.

Perez, I. M., B. W. LaFranchi, and R. C. Cohen: Nitrogen oxide chemistry in an urban plume: investigation of the chemistry of peroxy and multifunctional organic nitrates with a Lagrangian model, Atmos. Chem. Phys. Discuss., 9, 27099–27165, 2009.

Perring, A. E., S. E. Pusede, and R. C. Cohen: An observational perspective on the atmospheric impacts of alkyl and multifunctional nitrates on ozone and secondary organic aerosol, Chem. Reviews, 113, 5848–5870, doi:10.1021/cr300520x, 2013.

Pinho, P., C. Pio, and M. Jenkin: Evaluation of isoprene degradation in the detailed tropospheric chemical mechanism, MCM v3, using environmental chamber data, Atmos. Environ., 39, 1303–1322, 2005.

Roberts, J. M., and R. W. Fajer: UV absorption cross sections of organic nitrates of potential atmospheric importance and estimation of atmospheric lifetimes, Environ. Sci. Technol. 23, 945–951, 1989.

Sander, S. P., J. Abbatt, J. R. Barker, J. B. Burkholder, R. R. Friedl, D. M. Golden, R. E. Huie, C. E. Kolb, M. J. Kurylo, G. K. Moortgat, V. L. Orkin, and P. H. Wine: Chemical Kinetics and Photochemical Data for Use in Atmospheric Studies, Evaluation number 17, NASA Panel for data evaluation, JPL Publication 10-6, Jet Propulsion Laboratory, Pasadena, 2011 http://jpldataeval.jpl.nasa.gov.

Ren, X., J. R. Olson, J. H. Crawford, W. H. Brune, J. Mao, R. B. Long, Z. Chen, G. Chen, M. A. Avery, G. W. Sachse, J. D. Barrick, and G. S. Diskin, L. G. Huey, A. Fried, R. C. Cohen, B. Heikes, P. O. Wennberg, H. B. Singh, D. R. Blake, and R. E. Shetter : HOx chemistry during INTEX-A 2004: Observation, model calculation, and comparison with previous studies, J. Geophys. Res., 113, D05310, doi:10.1029/2007JD009166, 2008.

Sandu, A., and R. Sander: Technical Note: Simulating chemical systems in Fortran90 and Matlab with the Kinetic PreProcessor KPP-2.1, Atmos. Chem. Phys., 6, 187–195, 2006.

Saunders, S. M., M. E. Jenkin, R. G. Derwent, and M. J. Pilling: Protocol for the Development of the Master Chemical Mechanism, MCM v3 (Part A): tropospheric degradation of nonaromatic volatile organic compounds, Atmos. Chem. Phys., 3, 161–180, 2003, http://www.atmos-chem-phys.net/3/161/2003/.

Suarez-Bertoa, R., Picquet-Varrault, B., Tamas, W., Pangui, E., and Doussin, J.-F.: Atmospheric fate of a series of carbonyl nitrates: photolysis frequencies and OH-oxidation rate constants, Environ. Sci. Technol., 46, 12502–12509, 2012.

Vereecken, L., and J. Peeters: Decomposition of substituted alkoxy radicals - part I: a generalized structure-activity relationship for reaction barrier heights, Phys. Chem. Chem. Phys., 11, 9062–9074, 2009.

Wolfe, G. M., J. D. Crounse, J. D. Parrish, J.M. St. Clair, M. R. Beaver, F. Paulot, T. P. Yoon, P. O. Wennberg, and F. N. Keutsch: Photolysis, OH reactivity and ozone reactivity of a proxy for isoprene-derived hydroperoxyenals (HPALDs), Phys. Chem. Chem. Phys., 14, 7276–7286, 2012.

Xie, Y., F. Paulot, W. P. L. Carter, C. G. Nolte, D. J. Luecken, W. T. Hutzell, P. O. Wennberg, R. C. Cohen, and R. W. Pinder: Understanding the impact of recent advances in isoprene photooxidation on simulations of regional air quality, Atmos. Chem. Phys., 13, 8439–8455, 2013.

Table 1. Isoprene-derived carbonyl nitrates considered in this study.

Formula	Notation
nitrooxy ketones	
$CH_3COCH_2(ONO_2)$	NOA
$CH_3COCH(ONO_2)CH_2OH$	MVKNO3
$CH_3COCH(OH)CH_2ONO_2$	HMVKANO3
nitrooxy aldehydes	
$OCHCH_2(ONO_2)$	NO3CH2CHO
$OCHC(CH_3)(ONO_2)CH_2OH$	MACRNO3
nitrooxy enal	
$OCHCH=C(CH_3)CH_2ONO_2$	NC4CHO

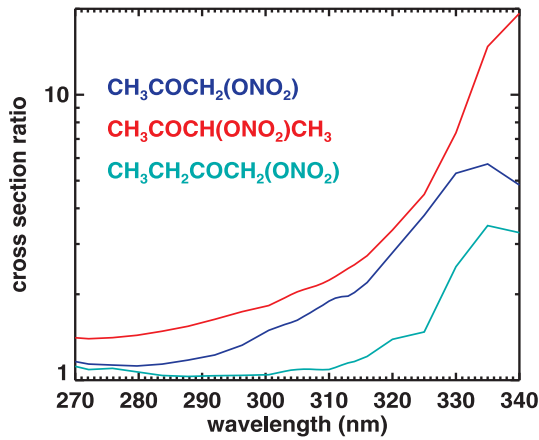**Fig. 1.** Cross section enhancement (r_{nk}) of several nitrooxy-ketones, i.e. ratio of their cross section (S_{nk}) to the sum of the cross sections of structurally similar monofunctional compounds $S_n + S_k$.
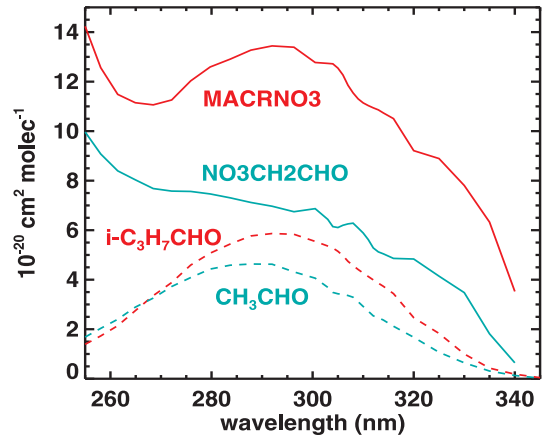

Fig. 2. Cross sections of acetaldehyde and i-butyraldehyde (dashed lines) recommended by Atkinson et al. (2006), and cross sections of ethanal nitrate (NO3CH2CHO) and MACRNO3 (cf. Table 1) estimated using Eq. 2 (solid lines).

Table 2. Isoprene-derived intermediates discussed in the text.

Formula	Notation
isoprenyl hydroxyperoxy radicals	
$HOCH_2C(CH_3)=CHCH_2O_2$	ISOPAO2
$CH_2=CHC(CH_3)(O_2)CH_2OH$	ISOPBO2
$HOCH_2CH=C(CH_3)CH_2O_2$	ISOPCO2
$CH_2=C(CH_3)CH(O_2)CH_2OH$	ISOPDO2
peroxy radicals from isoprenyl hydroxy nitrates	
$HOCH_2C(CH_3)(O_2)CH(OH)CH_2(ONO_2)$	INAO2
$HOCH_2C(ONO_2)(CH_3)CH(O_2)CH_2OH$	INB1O2
$HOCH_2CH(O_2)C(CH_3)(OH)CH_2(ONO_2)$	INCO2
$HOCH_2C(O_2)(CH_3)CH(ONO_2)CH_2OH$	INDO2

Table 3. Sink rates of carbonyl nitrates due to photolysis (J) and reaction with OH ($k_{OH} \cdot [OH]$), and overall lifetime $\tau = 1/(J + k_{OH} \cdot [OH])$. k_{OH} taken as the average of Neeb (2000) and MCMv3.2. $[OH] = 5 \cdot 10^6$ molec. cm^{-3}. Photolysis rates calculated with TUV for $30°$ solar zenith angle and 300 DU ozone. Hydroxy group effects in MVKNO3, MACRNO3 and HMVKANO3 photolysis were neglected in this calculation.
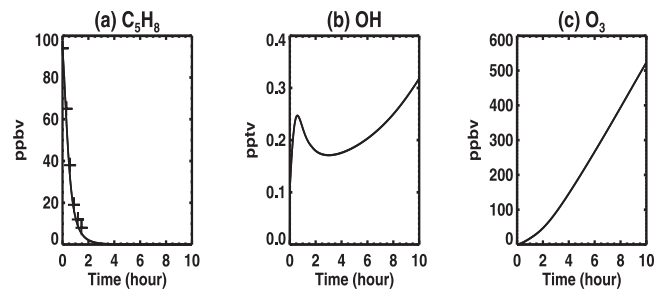

Fig. 3. Calculated mixing ratios of (a) isoprene, (b) OH, and (c) ozone in the experiment of Paulot et al. (2009). The reported measurements of isoprene are shown as black crosses.
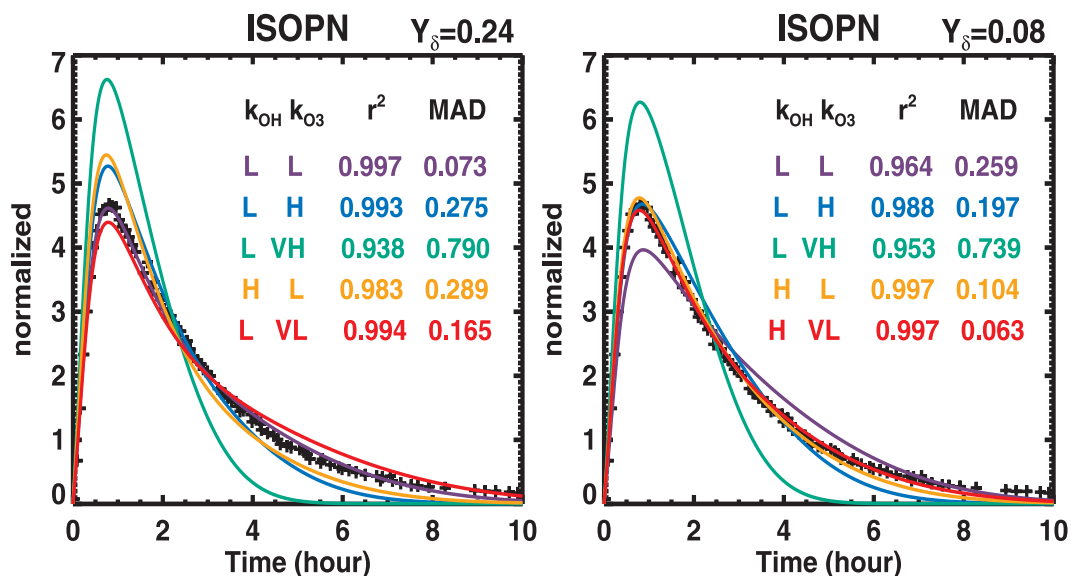
Compound	J (s^{-1})	$k_{OH} \cdot [OH]$ (s^{-1})	τ (hr)
NOA	$3.5 \cdot 10^{-5}$	$4 \cdot 10^{-6}$	7.1
MVKNO3	$5.6 \cdot 10^{-5}$	$8 \cdot 10^{-6}$	4.3
HMVKANO3	$3.2 \cdot 10^{-5}$	$1 \cdot 10^{-5}$	6.6
NO3CH2CHO	$1.5 \cdot 10^{-4}$	$1.2 \cdot 10^{-5}$	1.7
MACRNO3	$3.5 \cdot 10^{-4}$	$1.6 \cdot 10^{-5}$	0.76
NC4CHO	$5.6 \cdot 10^{-4}$	$2.1 \cdot 10^{-4}$	0.36

Fig. 4. Calculated mixing ratios of the normalized sum of first-generation isoprene nitrates weighted by their calibration factors in the experiment of Paulot et al. (2009). The reported measurements are shown as black crosses. The assumed nitrate yield in the reaction of δ-hydroxyperoxy radicals from isoprene is either 0.24 (left panel) or 0.08 (right). The model runs differ in the assumed reaction rates of isoprene β-hydroxynitrates with OH and O_3. The values for k_{OH} are $1.3 \cdot 10^{-11}$ (L) and $2.2 \cdot 10^{-11}$ (H) cm^3 molec.$^{-1}$ s^{-1}. The values for k_{O3} are $0.5 \cdot 10^{-17}$ (VL), 10^{-17} (L), $3 \cdot 10^{-17}$ (H) and $10.6 \cdot 10^{-17}$ (VH) cm^3 molec.$^{-1}$ s^{-1}. The (squared) Pearson's correlation coefficients and mean absolute deviations (MAD) are also indicated.
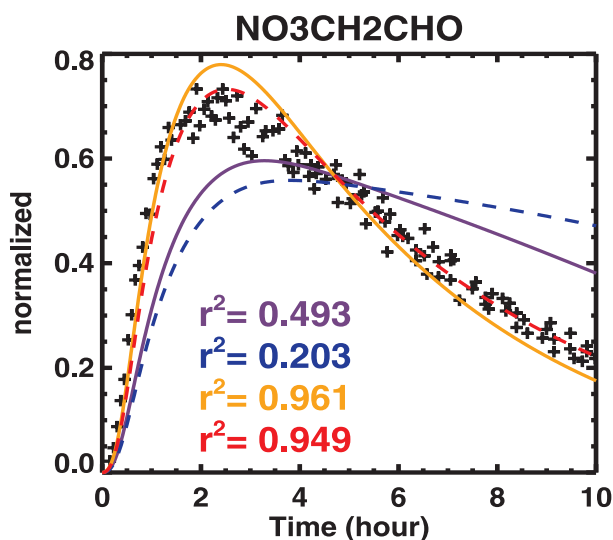

Fig. 5. Calculated mixing ratios of ethanal nitrate in the experiment of Paulot et al. (2009). The reported measurements are shown as black crosses. The model runs differ in the OH-reaction and photolysis rates. The OH-reaction rates are obtained either from the MCMv3.2 (full lines) or from Neeb (2000) (dashed lines). Indigo and blue curves: MCM photolysis; orange and red: fast photolysis as described in this article.
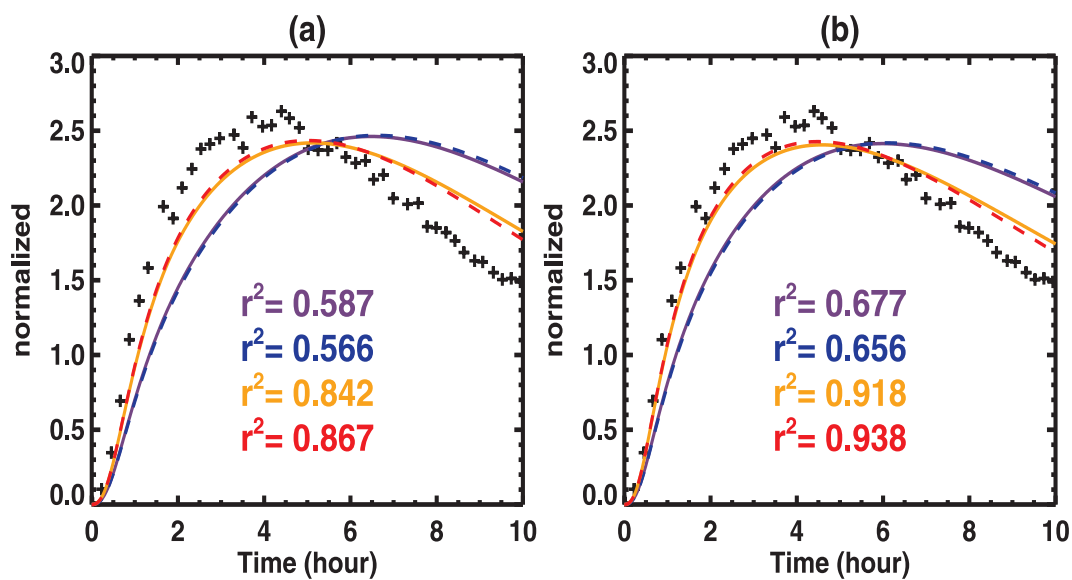
Fig. 6. Calculated mixing ratios of the normalized sum of MVKNO3 and isomers (HMVKANO3 and MACRNO3) in the experiment of Paulot et al. (2009). The reported measurements are shown as black crosses. The assumed OH-reaction rate of the isoprene β-hydroxynitrates is either (a) $1.3 \cdot 10^{-11}$ (left) or (b) $2.2 \cdot 10^{-11}$ cm^3 molecule^{-1} s^{-1} (right). The model runs further differ in the OH-reaction and photolysis rates of the carbonyl nitrates. Indigo and blue curves: MCM photolysis; orange and red: fast photolysis as described in this article. The OH-reaction rates are obtained either from the MCMv3.2 (full lines) or from Neeb (2000) (dashed lines). The (squared) Pearson's correlation coefficients are also indicated.